Human TCR-Binding Affinity Is Governed by MHC Class Restriction[1]

David K. Cole,*‡ Nicholas J. Pumphrey,† Jonathan M. Boulter,‡ Malkit Sami,† John I. Bell,* Emma Gostick,* David A. Price,* George F. Gao,*§ Andrew K. Sewell,*‡ and Bent K. Jakobsen[2†]

T cell recognition is initiated by the binding of TCRs to peptide-MHCs (pMHCs), the interaction being characterized by weak affinity and fast kinetics. Previously, only 16 natural TCR/pMHC interactions have been measured by surface plasmon resonance (SPR). Of these, 5 are murine class I, 5 are murine class II, and 6 are human class I-restricted responses. Therefore, a significant gap exists in our understanding of human TCR/pMHC binding due to the limited SPR data currently available for human class I responses and the absence of SPR data for human class II-restricted responses. We have produced a panel of soluble TCR molecules originating from human T cells that respond to naturally occurring disease epitopes and their cognate pMHCs. In this study, we compare the binding affinity and kinetics of eight class-I-specific TCRs (TCR-Is) to pMHC-I with six class-II-specific TCRs (TCR-IIs) to pMHC-II using SPR. Overall, there is a substantial difference in the TCR-binding equilibrium constants for pMHC-I and pMHC-II, which arises from significantly faster on-rates for TCRs binding to pMHC-I. In contrast, the off-rates for all human TCR/pMHC interactions fall within a narrow window regardless of class restriction, thereby providing experimental support for the notion that binding half-life is the principal kinetic feature controlling T cell activation. ***The Journal of Immunology,*** **2007, 178: 5727–5734.**

On the cell surface, $\alpha\beta$ T cells recognize foreign Ags by means of an interaction dominated by the specific binding of the $\alpha\beta$ TCR to short peptide fragments complexed with MHCs (pMHC)[3] (1, 2). There are two main subpopulations of $\alpha\beta$ T cells: CTL, which generally recognize intracellularly derived antigenic peptides in the context of MHC class I (MHC-I) (3, 4), and Th lymphocytes (Th cells), which generally recognize exogenously derived antigenic peptides in the context of MHC class II (MHC-II) (5, 6). MHC-I presents shorter peptides, typically 8–12 aa in length, bound in a groove formed by the α1 and α2 domains (7). CTLs, which usually express the coreceptor CD8, mediate direct cell killing of cells infected with intracellular pathogens and tumor cells (8). MHC-II presents longer peptides, typically 10–25 aa in length, in a binding groove formed between the α1 and β1 domains (9). Th cells, which generally express the CD4 coreceptor, typically respond to pMHC-II by producing soluble factors that "help" both innate and adaptive immune reactions (10, 11).

Through somatic gene rearrangement, the immune system produces a vast variety of random TCR specificities, including self-Ag reactive and nonreactive receptors (1, 12). Thymic selection narrows the peripheral TCR repertoire, eliminating cells with inept or autoreactive receptors. Thus, the peripheral populations of T cells express receptors that have the potential to recognize foreign peptides in the context of self-MHC (13). The accumulated evidence derived from studies with soluble TCRs indicates that TCR/pMHC affinities of Ag-responsive T cells fall within a narrow range (14). This affinity range is thought to represent a compromise, allowing T cells to successfully respond to antigenic peptides, while remaining tolerant to autoantigens (15). Further evidence has indicated that the half-life, or off-rate, of this interaction must fall within a specific "window" to enable intracellular signal transduction while being brief enough to allow each pMHC complex to be engaged by multiple TCRs in series (16). This enables the required number of TCR/pMHC induced triggering events to take place in order for T cell activation to occur (17).

The affinity range reported for TCRs binding to agonist pMHCs is K_D ~1–50 μM (18). This is considerably weaker than most other protein-protein interactions of biological consequence (18, 19). Interestingly, studies reported so far indicate that CTL-derived TCRs (TCR-I), which are specific for pMHC-I, bind with stronger affinities than Th cell-derived TCRs (TCR-II), which bind to pMHC-II (18). However, the critical parameter determining the T cell activation threshold is likely to be the off-rate, i.e., the duration of TCR/pMHC engagement. This is exemplified by the demonstration that, of two ligands with similar K_D, only the one with a slow off-rate acts as an agonist (20, 21). To date, these principles are based primarily on a limited number of murine TCR/pMHC interactions, measured using a range of methods. Only six natural human TCR/pMHC-I interactions have been measured, with no data available for human TCR/pMHC-II (Table I). Therefore, a

*Nuffield Department of Clinical Medicine, John Radcliffe Hospital, University of Oxford, Oxford, United Kingdom; †Avidex Limited, Abingdon, Oxon, United Kingdom; ‡Department of Medical Biochemistry and Immunology, School of Medicine, Cardiff University, Cardiff, United Kingdom; and §Center for Molecular Immunology, Institute of Microbiology, Chinese Academy of Sciences, Beijing, People's Republic of China

Received for publication December 7, 2006. Accepted for publication February 12, 2007.

The costs of publication of this article were defrayed in part by the payment of page charges. This article must therefore be hereby marked *advertisement* in accordance with 18 U.S.C. Section 1734 solely to indicate this fact.

[1] D.K.C. was supported by a Medical Research Council (MRC) (U.K.) studentship. G.F.G. was supported by Chinese Academy of Sciences Knowledge Innovation Project Grant No. KSCX2-SW-227. J.M.B. was supported by a Research Councils UK academic fellowship. D.A.P. is an MRC Senior Clinical Fellow; A.K.S. is a Wellcome Trust Senior Fellow.

[2] Address correspondence and reprint requests to Dr. Bent K. Jakobsen, Avidex Limited, 57C Milton Park, Abingdon, Oxon, OX14 4RX, U.K. E-mail address: bent.jakobsen@avidex.com

[3] Abbreviations used in this paper: pMHC, peptide-MHC; MHC-I, MHC class I; MHC-II, MHC class II; β_2m, β_2-microglobulin; SPR, surface plasmon resonance; MBP, myelin basic protein.

Table I. *Previously published TCR/pMHC measurements*[a]

Interaction[b]	K_D (μM)	K_{on} ($M^{-1}s^{-1}$)	K_{off} (s^{-1})
TCR/pMHC I (murine)			
F5 TCR/H2-D^b Flu (28)	7	3×10^4	0.2
2C TCR/H2-L^d p2Ca (41)	1.6	9.4×10^3	0.015
42.12 TCR/H2-K^b OVA (42)	7	3×10^3	0.02
T1 TCR/H2-K^d PbCS (43)	4	ND	ND
BM3.3 TCR/H2-K^b pBM1 (44)	2.6	ND	ND
TCR/pMHC II (murine)			
2B4 TCR/I-E^k MCC (40)	6	4×10^3	0.02
3.L2 TCR/I-E^k Hb (45)	10	6×10^3	0.06
172.10 TCR/I-A^u MBP (46)	6	4×10^4	0.2
1934.4 TCR/I-A^u MBP (46)	30	5×10^3	0.2
D10 TCR/I-A^k CA (5)	7	6×10^3	0.05
TCR/pMHC I (human)			
A6 TCR/HLA-A2 Tax (27)	1	1×10^5	0.1
JM22 TCR/HLA-A2 Flu (28)	6	4×10^4	0.2
IG4/HLA-A2 NYESO (47)	13	1.2×10^4	0.17
SB27 TCR/HLA-B35 EBV (48)	9.9	9.3×10^3	0.13
LC13 TCR/HLA-B8 EBNA (26)	12.5	3.5×10^4	0.39
G10 TCR/HLA-A2 HIV-gag (49)	2.2	3.3×10^4	0.06

[a] Previously published TCR/pMHC affinity measurements of murine TCR/pMHC I interactions, murine TCR/pMHC II interactions, and human TCR/pMHC I interactions.
[b] Reference numbers in parentheses.

direct comparison of the binding affinity and kinetics of class I- and class II-restricted human TCR responses has previously been impossible. To address this issue, we report here the first comparative study of a spectrum of naturally selected human TCR affinities and kinetics, comparing binding to both MHC-I and MHC-II complexed with pathogenic, tumor, and self peptide Ags (Table II).

Materials and Methods

Generation of expression plasmids

The TCR and the MHC sequences were generated by PCR mutagenesis (Stratagene) and PCR cloning. All sequences were confirmed by automated DNA sequencing (Lark Technologies). For each TCR, a disulphide-linked construct was used to produce the soluble domains (variable and constant) for both the α- and β-chains (22, 23). The MHC-I soluble α-chains (α1-, α2-, and α3-chain domains), tagged with a biotinylation sequence, and β_2-microglobulin (β_2m) were also cloned and used to make the MHC-I proteins. The TCR, MHC-I, and β_2m sequences were inserted into separate pGMT7 expression plasmids under the control of the T7 promoter (22). For the MHC-II proteins, the soluble domains of the α-chain (containing a biotinylation sequence tag and a C-terminal FOS leucine zipper) and β-chains (containing the peptide sequence attached via an N-terminal flexible linker and a C-terminal JUN leucine zipper) were cloned (24). The pMHC-II sequences were inserted into the pAcAB3 vector for baculoviral expression.

Protein expression, refolding, and purification

Competent Rosetta DE3 *Escherichia coli* cells were used to produce the TCR-I and TCR-II fragments (α- and β-chains), and the MHC-I α and β_2m chains in the form of inclusion bodies using 0.5 mM isopropyl β-D-thiogalactoside to induce expression as described previously (22). For a 1-L refold, 30 mg of TCR α-chain inclusion bodies were incubated at 37°C for 15 min with 10 mM DTT and added to cold refold buffer (50 mM Tris (pH 8.1), 2 mM EDTA, 2.5 M urea, 6 mM cysteamine hydrochloride and 4 mM cystamine). After 10–15 min, 30 mg of TCR β-chain, incubated for 10–15 min at 37°C with 10 mM DTT, was added. For a 1-L pMHC-I refold, 30 mg of α-chain was mixed with 30 mg of β_2m and 4 mg of synthetic peptide at 37°C for 15 min. This was then added to cold refold buffer (50 mM Tris (pH 8), 2 mM EDTA, 400 mM L-arginine, 6 mM cysteamine hydrochloride and 4 mM cystamine). Refolds were mixed at 4°C for >1 h. Dialysis was conducted against 10 mM Tris (pH 8.1) until the conductivity of the refolds was under 2 mS/cm. The refolds were then filtered, ready for purification steps. The refolded proteins were purified initially by ion exchange using

Table II. *Origin and details of TCRs and pMHC epitopes*[a]

	Ag Origin	MHC Epitope
TCR-I[b]		
AM3 (50)	EBV	A*2402 EBV (PYLFWLAAI)
LC13 (51)	EBV	B*0801 EBNA (FLRGRAYGL)
gp100 (52)	Melanoma	A*0201 gp100 (YLEPGPVTV)
JM22 (53)	Influenza	A*0201 Flu (GILGFVFTL)
TEL	Telomerase	A*0201 Tel (ILAKFLHWL)
A6 (54)	HTLV	A*0201 Tax (LLFGYPVYV)
GRB (55, 56)	Influenza	B*2705 Flu (SRYWAIRTR)
MEL	Melanoma	A*0201 Mel A (ELAGIGILTV)
TCR-II		
AH1.23 (57)	*Chlamydia trachomatis*	DRβ*0401 C-HSP (GRHVVIDKSFGSPQIT)
HA1.7 (58)	Influenza	DRβ*0101 and DRβ*0401 HA (PKYVKQNTLKLAT)
MAW 13 (59)	*Mycobacterium leprae*	DRβ*0301 M-HSP (MAKTIAYDEEARRGL)
2E11 (60)	Myelin basic protein	DRβ*1501 MBP (ENPVVHFFKNIVTPR)
1A12 (60)	Myelin basic protein	DRβ*1501 MBP (ENPVVHFFKNIVTPR)

[a] Origin and details of TCRs and pMHC epitopes used (DRα1*0101 was used for all of the pMHC-II proteins). All TCRs originated from T cell clones that respond to naturally occurring Ags.
[b] Reference numbers in parentheses.

Table III. *Equilibrium data at 25°C with SD* ($n = 3$)

	K_D μM
TCR-I/pMHC-I	
gp100 TCR/A2 gp100	11 ± 0.5
TEL TCR/A2 Tel	34 ± 2
LC13 TCR/B8 EBNA	9 ± 0.4
AM3 TCR/A24 EBV	21 ± 0.8
JM22 TCR/A2 Flu	5 ± 0.2
A6 TCR/A2 Tax	2 ± 0.7
GRB TCR/B27 Flu	6 ± 0.1
MEL TCR/A2 Mel	18 ± 1
TCR-II/pMHC-II	
MAW13 TCR/DR3 M-HSP	25 ± 0.5
AH1.23 TCR/DR4 C-HSP	28 ± 1
1A12 TCR/DR2 MBP	69 ± 4
2E11 TCR/DR2 MBP	112 ± 5
HA1.7 TCR/DR0101 HA	37 ± 1
HA1.7 TCR/DR0401 HA	40 ± 3
Average TCR-I/pMHC-I K_D	13 ± 11
Average TCR-II/pMHC-II K_D	52 ± 33

a Poros50HQ column. Soluble MHC-II proteins were produced as previously described (24). The expressed proteins were purified initially by affinity chromatography using L243 Ab immobilized onto CNBr Sepharose 4B. They were then ion exchanged using a Poros50HQ column, and finally gel filtered into BIAcore buffer (10 mM HEPES (pH 7.4), 150 mM NaCl, 3 mM EDTA and 0.005% (v/v) Surfactant P20), using a Superdex200HR column. This step was implemented on the day of analysis. Protein quality was analyzed by Coomassie-stained SDS-PAGE.

pMHC biotinylation

Biotinylated pMHC was prepared as previously described (25).

Surface plasmon resonance (SPR) equilibrium analysis

The binding analysis was performed using a BIAcore 3000 equipped with a CM5 sensor chip as previously reported (25). Except for the A24 EBV experiment at 15°C, in which 2000 response units were added, between 200 and 400 response units of biotinylated pMHC complexes were immobilized to streptavidin, which was chemically linked to the chip surface. The pMHC was injected at a slow flow rate (10 μl/min) to ensure a uniform distribution of pMHC on the chip surface. Combined with the small amount of pMHC bound to the chip surface, this reduced the likelihood of mass transfer being in effect during these experiments. TCRs were purified and concentrated to a ~100 μM on the same day of SPR analysis to reduce the likelihood of TCR aggregation affecting the results. For equilibrium analysis, 10 serial dilutions were carefully prepared in triplicate for each sample and injected over the relevant sensor chips at 25°C. All experiments were conducted in triplicate using the same chip on the same day. Results were analyzed using BIAevaluation 3.1, Microsoft Excel, and Origin 6.1. The equilibrium-binding constant (K_D) values were calculated using a nonlinear curve fit ($y = (P_1x)/(P_2 + x)$). The binding of the HA1.7 TCR to HLA DR1-HA made in insect cells and protein made using an *E.coli* expression system was identical (data not shown) and suggests that the carbohydrate added to the MHC in the insect expression system has no effect on the binding of soluble TCR.

SPR kinetic analysis

Experiments were conducted to determine the K_{on} and K_{off} values for each sample at 25°C. Chip and reagent preparation was conducted identically to the equilibrium analysis. The TCRs were concentrated to ~100 μM and six to eight serial dilutions were injected onto the chip at 30 μl/min and measured in triplicate. The response was measured over a 45–60 s injection with a 30–150 s dissociation period. The K_{on} and K_{off} values were calculated assuming 1:1 Langmuir binding and the data were analyzed using a global fit algorithm (BIAevaluation 3.1).

SPR temperature-dependent equilibrium and kinetic analysis

To compare the effect of temperature on TCR-binding affinity (K_D) and kinetics (K_{on} and K_{off}) for pMHC-I and pMHC-II, analyses were conducted at 15°C and 37°C using the same experimental setup as at 25°C.

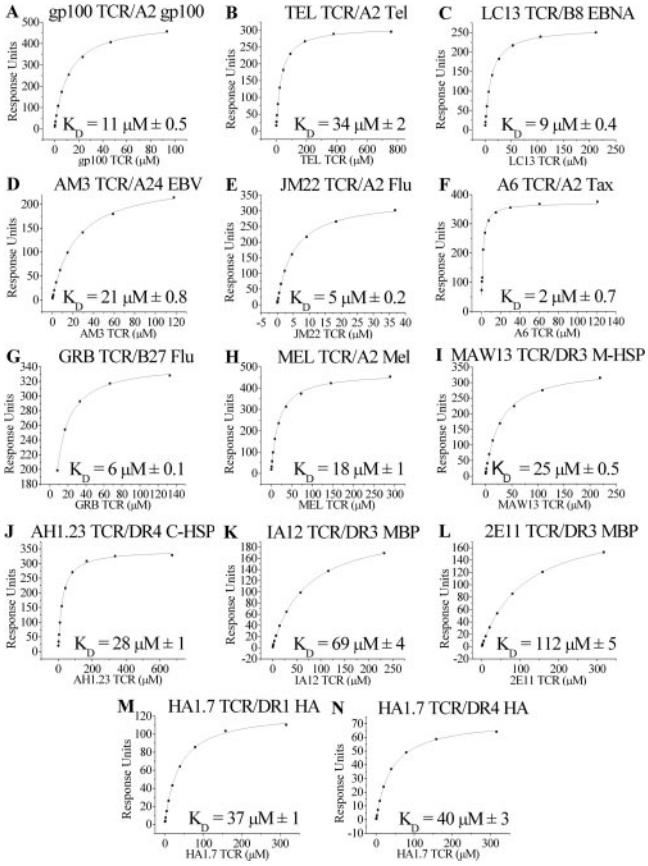

FIGURE 1. Equilibrium-binding analysis at 25°C. *a–h*, TCR-I equilibrium-binding responses to their cognate pMHC-I. *i–n*, TCR-II equilibrium-binding responses to their cognate pMHC-II. Ten serial dilutions were conducted in triplicate for each equilibrium experiment. The average response for each concentration is plotted with SD ($n = 3$). The equilibrium-binding constant (K_D) values are plotted using a nonlinear curve fit ($y = (P_1x)/(P_2 + x)$).

Statistical analysis

A two-tailed Student *t* test using equal variance (calculated using an F test) was performed to analyze the actual difference between the two means (TCR-I vs TCR-II) in relation to the variation in the data for statistical relevance using Microsoft Excel XP. This test was used to compare the difference in K_D between TCR-I ($n = 8$) and TCR-II ($n = 6$) as well as the difference in K_{on} and K_{off} values between TCR-I ($n = 7$) and TCR-II ($n = 4$). Relevant *p* values are given in the main text.

Results

Class I-restricted TCRs bind with greater affinity than class II-restricted TCRs

Binding data was collected for eight TCR-I/pMHC-I and six TCR-II/pMHC-II interactions. SPR was used to determine the equilibrium K_D of each TCR for its cognate pMHC (Table III). Experiments at 25°C showed that TCR-I bind (Fig. 1, *a–h*) within a higher affinity range than TCR-II (Fig. 1, *i–n*) (Table III). The K_D calculated for the binding of the A6, JM22, and LC13 TCRs to A2 Tax, A2 Flu, and B8 EBNA, respectively, have been previously measured (26–28); the data presented here (Table III) are in good agreement with those values (Table I). The average K_D for TCR-I was 13 ± 11 μM, compared with an average TCR-II K_D of 52 ± 33 μM. This represents a significantly greater average affinity for TCR-I binding than TCR-II binding ($p_{value} = 0.009$).

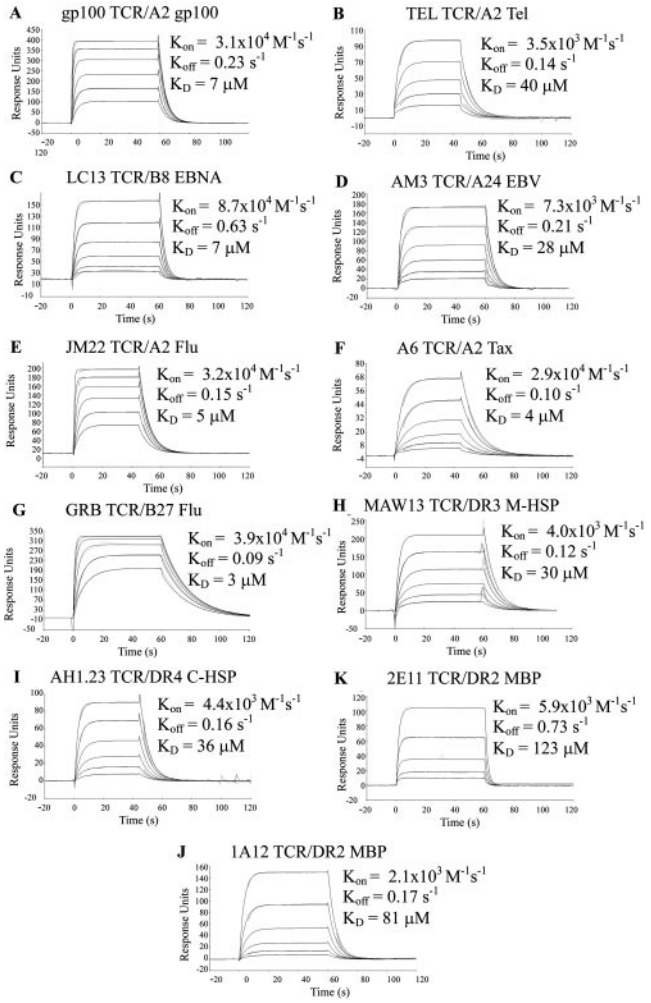

FIGURE 2. Kinetic-binding analysis at 25°C. *a–g*, TCR-I kinetic-binding responses to their cognate pMHC-I. *h–k*, TCR-II kinetic-binding responses to their cognate pMHC-II. Six to eight serial dilutions of concentrated TCR were injected at 30 μl/min for between 45 and 60 s association periods. Each binding response was calculated assuming 1:1 Langmuir binding and the data were analyzed using a global fit algorithm (BIAevaluation 3.1) to calculate K_{on} and K_{off} values. Both the data and the global fit analyses are shown as solid lines for each response, although the quality of the fit makes this difficult to see in some cases.

The effect of Ag origin on TCR binding

Five of the TCR-I responses are specific for virally derived Ags, while three are specific for tumor Ags; two TCR-II responses are specific for self Ags, while four are specific for bacterially derived Ags. Antiviral TCR-Is bound to their cognate Ags (A2 Tax, A24 EBV, B27 Flu, B8 EBNA, and A2 Flu) with an average K_D of 9 ± 7 μM. In comparison, TCR-I specific for the tumor-associated antigenic peptides (A2 Mel, A2 gp100, and A2 Tel), bound with an average K_D of 21 ± 12 μM. Antibacterial TCR-II bound their cognate Ags (DR3 M-HSP, DR4 C-HSP, DR1 HA, and DR4 HA) with an average K_D of 33 ± 8 μM, and TCR-II specific for the self Ag DR2 myelin basic protein (MBP) bound with an average K_D of 91 ± 30 μM. Thus, a similar affinity hierarchy is observed within both TCR-I and TCR-II, dependent on the antigenic origin (pathogenic>tumor/self).

TCR binding to pMHC I and II is governed by K_{on}

Kinetic-binding analyses were conducted at 25°C to measure the on-rate (K_{on}) and off-rate (K_{off}) for each interaction. The most salient feature to emerge was the similarity in K_{off} values for all TCRs regardless of MHC-I or MHC-II restriction. The average TCR-I K_{off} was 0.22 ± 0.19 s^{-1} vs an average TCR-II K_{off} of 0.30 ± 0.29 s^{-1}. In contrast, the average K_{on} for TCR-I interactions was $3.3 \times 10^4 \pm 2.9 \times 10^4$ $M^{-1}s^{-1}$ compared with a K_{on} of $4.1 \times 10^3 \pm 1.3 \times 10^3$ $M^{-1}s^{-1}$ for TCR-II. Consequently, there is a significant difference in the average K_{on} between TCR-I (Fig. 2, *a–g*) and TCR-II (Fig. 2, *h–k*) ($p_{value} = 0.01$), compared with an insignificant difference in K_{off} ($p_{value} = 0.62$) (Table IV). This does not challenge the concept of a narrow range of K_{off} values being the key binding parameter controlling TCR-mediated signal transduction, as suggested, for example, by the T cell kinetic proof reading hypothesis (29).

The effect of temperature on TCR/pMHC-binding affinity

Equilibrium and kinetic-binding analyses were also performed at 15°C and 37°C on a selection of TCR-I and TCR-II interactions due to the rapid kinetics attributed to TCR/pMHC binding (25, 28). Slowing down the TCR/pMHC interaction provided the advantage of allowing a greater number of data points to be collected for the K_{on} and K_{off} values (Table V), adding to the potential accuracy of the results. For the TCR-I and TCR-II interactions, the K_{on} and K_{off} values were, on average, ~2-fold slower at 15°C than at 25°C and confirmed the above findings (Figs. 3 and 4). Additional experiments were conducted at physiological temperature (37°C) both to expand the data in terms of temperature effect on TCR/pMHC binding and to examine the interactions under physiological conditions (Fig. 5). Accurate detection of the on- and off-rates of the TCR/pMHC interactions were beyond the limits of the BIAcore 3000 due the rapid kinetics observed at 37°C. However, the K_D values obtained using equilibrium analyses were virtually identical with those obtained at 15°C and 25°C (Table VI). Therefore, differences in temperature significantly change the kinetics, but not the affinity, of TCR/pMHC interactions investigated in this analysis.

Discussion

Class I-restricted TCRs bind with greater affinity than class II-restricted TCRs

In this study, we directly show, for the first time, that human TCRs bind to pMHC-I with approximately five times greater affinity than to pMHC-II. This study also represents the first binding affinity and kinetic data of human TCR/pMHC-II interactions. Previous binding data for TCR/pMHC interactions have emanated from a number of different laboratories and groups, derived from both mouse and human origin, in which a standardized method for SPR analysis is not always possible. These factors have limited the direct comparison of TCR binding to pMHC-I and pMHC-II. In this study, an identical method was used, wherever possible, to produce the TCR and pMHC proteins, and to perform the biophysical analysis. To further add to the accuracy and reproducibility of this study, we have repeated some human TCR/pMHC-I-binding data, which had been previously published (LC13 TCR/B8 EBNA, JM22 TCR/A2 Flu, and A6 TCR/A2 Tax) with virtually identical results. The difference observed between human TCR binding to pMHC-I and pMHC-II is also mirrored in the murine system, where accumulated evidence (Table I) indicates that the average murine TCR/pMHC-I affinity is K_D = 4 μM, compared with the average murine TCR/pMHC-II affinity, which is K_D = 12 μM. This 3-fold difference is consistent with the human data presented. This also indicates that murine TCRs bind generally more strongly compared with human TCRs (average human TCR/pMHC-I affinity is K_D = 13 μM, average human TCR/pMHC-II affinity is

Table IV. *Kinetic data at 25°C*[a]

	K_{on} $M^{-1}s^{-1}$	K_{off} s^{-1}	K_D μM (K_{off}/K_{on})
TCR-I/pMHC-I			
gp100 TCR/A2 gp100	3.1×10^4	0.23	7
TEL TCR/A2 Tel	3.5×10^3	0.14	40
LC13 TCR/B8 EBNA	8.7×10^4	0.63	7
AM3 TCR/A24 EBV	7.3×10^3	0.21	28
JM22 TCR/A2 Flu	3.2×10^4	0.15	5
A6 TCR/A2 Tax	2.9×10^4	0.10	4
GRB TCR/B27 Flu	3.9×10^4	0.09	3
MEL TCR/A2 Mel	$>1 \times 10^6$	>1	nm
TCR-II/pMHC-II			
MAW13 TCR/DR3 M-HSP	4.0×10^3	0.12	30
AH1.23 TCR/DR4 C-HSP	4.4×10^3	0.16	36
1A12 TCR/DR2 MBP	2.1×10^3	0.17	81
2E11 TCR/DR2 MBP	5.9×10^3	0.73	123
HA1.7 TCR/DR1 HA	$>1 \times 10^6$	>1	nm
HA1.7 TCR/DR4 HA	$>1 \times 10^6$	>1	nm
Average TCR-I/pMHC-I	$3.3 \times 10^4 \pm 2.9 \times 10^4$	0.22 ± 0.19	13 ± 15
Average TCR-II/pMHC-II	$4.1 \times 10^3 \pm 1.3 \times 10^3$	0.30 ± 0.29	68 ± 43

[a] nm, Not measurable, i.e. the kinetics were too fast to accurately determine.

$K_D = 52$ μM). This could indicate a fundamental difference in the way that murine TCRs "see" Ag compared with the human system, although the number of TCR/pMHC interactions presently available is too small to determine whether this observation is universal. In support of this idea is the observation that human CD8 binds to pMHC-I with three to four times weaker affinity compared with murine CD8, virtually identical with the difference in affinity observed between murine and human TCR/pMHC interactions (25, 30, 31). Similarly, binding data for the CD4 coreceptor indicates that it binds considerably weaker (K_D >200 μM) than the CD8 coreceptor. This could be important to maintain the binding affinity ratio between CD4/pMHC-II and the TCR/pMHC-II interaction, which we have shown to be of weaker affinity than TCR binding to pMHC-I. These differences could represent a fundamental biological necessity for the binding affinity ratio between the TCR/pMHC interaction and the coreceptor/pMHC in maintaining Ag specificity vs T cell activation.

The difference in affinity observed between human TCR-I and TCR-II indirectly supports a number of possible implications for T cell function. For example, a greater TCR-I-binding affinity could potentially result in a stronger CTL-mediated activation signal, compared with Th cells, due to a greater number of TCR/pMHC-I interactions occurring. This suggests either that Th cells have a lower T cell activation threshold compared with CTLs, or that the signal mediated by TCR-II is stronger than TCR-I to compensate for the difference in the number of TCR/pMHC interactions. However, under cellular conditions, there are a number of other factors that contribute to T cell activation. First, more efficient serial triggering may occur with TCRs exhibiting weaker affinity. This is because weaker binding could allow such TCRs to contact multiple pMHC molecules in series more quickly than TCRs with greater affinity (16). Second, T cells expressing TCRs with lower binding affinities could possess a higher density of TCRs on their cell surface, or could respond to cells expressing a higher concentration of Ag, creating a greater number of weaker signals compared with T cells with higher affinity TCR/pMHC interactions (32). Finally, the function and expression of the coreceptors CD4 and CD8, which have been shown to increase Ag sensitivity, could be important in T cells with weaker binding TCRs (30, 33). This is further supported by studies showing that CTLs responding to Ags that bind TCRs weakly have a greater degree of dependence on CD8 activity compared with CTLs responding to Ags that bind TCRs more strongly (B. Laugel, H. van der Berg, E. Gostick, D. K. Cole, L. Wooldridge, J. M. Boulter, A. Milicic, D. A. Price, and A. K. Sewell, manuscript in preparation).

Anti-pathogen TCRs bind with highest affinity

These results suggest that TCRs specific for pathogenic Ags such as those derived from viruses and bacteria could bind with stronger affinity compared with nonpathogenic, tumor and self, Ags, although this is limited by the small number of interactions measured for each type of Ag. Immune responses to pathogenic Ags are thought to elicit much stronger reactions compared with nonpathogenic Ags. It is therefore tempting to suggest that a link exists

Table V. *Kinetic and equilibrium analysis data at 15°C*

	K_{on} $M^{-1}s^{-1}$	K_{off} s^{-1}	K_D μM (K_{off}/K_{on})	K_D μM
TCR-I/pMHC-I				
gp100 TCR/A2 gp100	1.4×10^4	0.09	6	9 ± 0.1
TEL TCR/A2 Tel	1.0×10^3	0.05	48	44 ± 3
LC13 TCR/B8 EBNA	4.1×10^4	0.32	8	8 ± 0.3
AM3 TCR/A24 EBV	3.4×10^3	0.08	24	17 ± 1
JM22 TCR/A2 Flu	1.8×10^4	0.03	1	2 ± 0.1
A6 TCR/A2 Tax	1.5×10^4	0.05	3	3 ± 0.3
TCR-II/pMHC-II				
MAW13 TCR/DR3 M-HSP	1.7×10^3	0.06	33	28 ± 0.8
AH1.23 TCR/DR4 C-HSP	1.5×10^3	0.09	59	42 ± 1
1A12 TCR/DR2 MBP	4.7×10^3	0.05	107	96 ± 2

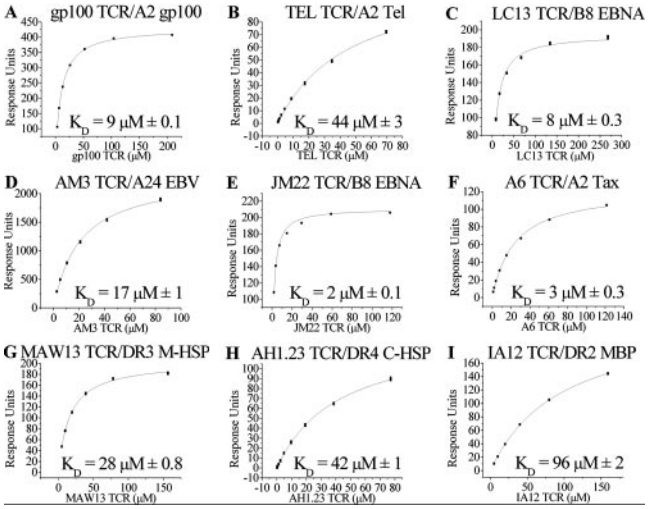

FIGURE 3. Equilibrium-binding analysis (15°C). *a–f*, TCR-I equilibrium-binding responses to their cognate pMHC-I. *g–i*, TCR-II equilibrium-binding responses to their cognate pMHC-II. Six to eight serial dilutions were conducted in triplicate for each equilibrium experiment. The average response for each concentration is plotted with SD ($n = 3$). The equilibrium-binding constant (K_D) values are plotted using a nonlinear curve fit ($y = (P_1x)/(P_2 + x)$).

between Ag potency and TCR affinity, with strongly binding TCRs eliciting a stronger immune response.

TCR-I and TCR-II have different on-rates, but similar off-rates

The significantly faster on-rates for TCR-I, compared to TCR-II, are indicative of a higher degree of conformational flexibility and higher entropic cost upon binding for the TCR-II interactions. A possible explanation for this observation can be construed from the crystal structures of pMHC-I and II. Although the total number of TCR accessible residues is similar in both pMHC-I and II Ag presentation, the MHC-II peptide conformation is potentially less favorable for TCR binding. This is because the MHC-II peptides are more buried within the $\alpha1/\beta1$ binding groove and, compared with MHC-I peptide presentation, have an overall "flatter" topology (34). In the case of MHC-I peptide presentation, a prominent central bulge in the peptide, away from the MHC-I surface, is a common conformational feature and provides TCR-I with a far more exposed motif with which to bind (34, 35). Furthermore, TCR-II must be able to recognize a theoretically greater range of Ags than TCR-I, due to the longer length of the peptides and the greater degree of variability therein (36). A slow K_{on} could be indicative of a lower degree of specificity for TCR-II, supported by the observed higher degree cross-reactivity for Th cells compared with CTLs (37).

K_{off} is a measure of the stability of a protein-protein interaction. These data show that there is no significant difference between the average K_{off} value for TCR binding to pMHC-I or pMHC-II. This observation is supported by TCR/pMHC complex crystal structures, which show that the number of molecular contacts is relatively conserved for TCR-I and II binding (34). Theoretically, for TCR-mediated activation signals to occur, the half-life of the interaction must be sufficient for activation signals to take place, a notion supported by investigations showing that fast K_{off} can lead to T cell anergy, and extremely fast K_{off} can result in T cell antagonism (38). This suggests that, because the K_{off} of the TCR binding to pMHC-I and pMHC-II is conserved, the half-life could be an important functional determinant for T cell activation.

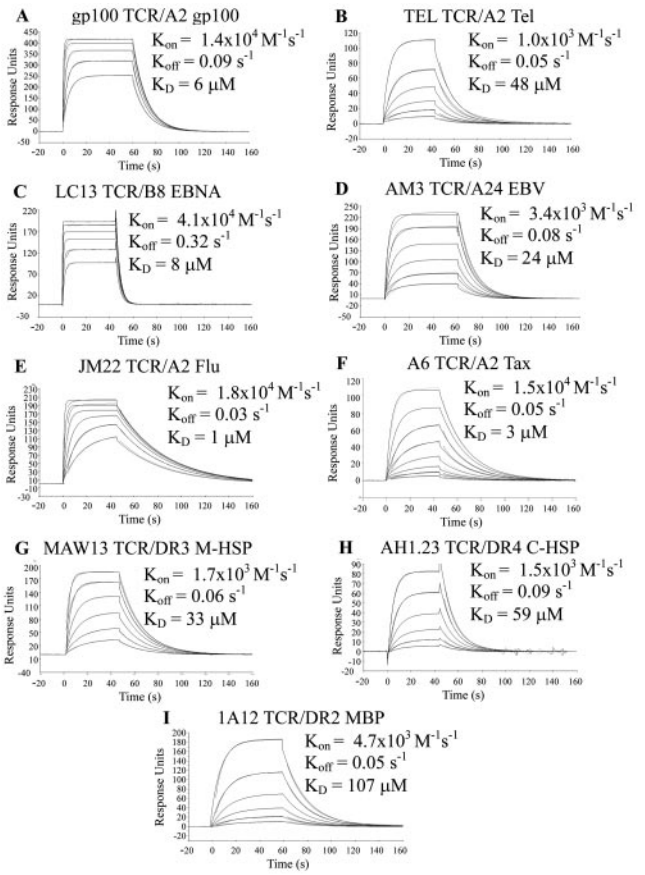

FIGURE 4. Kinetic-binding analysis at 15°C. *a–f*, TCR-I kinetic-binding responses to their cognate pMHC-I. *g–i*, TCR-II kinetic-binding responses to their cognate pMHC-II. Six to eight serial dilution of concentrated TCR were injected at 30 μl/min for between 45 and 60 s association periods. Each binding response was calculated assuming 1:1 Langmuir binding and the data were analyzed using a global fit algorithm (BIAevaluation 3.1) to calculate K_{on} and K_{off} values. Both the data and the global fit analyses are shown as solid lines for each response, although the quality of the fit makes this difficult to see in some cases.

Conclusions

This first comparative study of naturally selected human TCR/pMHC interactions has revealed three fundamental features. First,

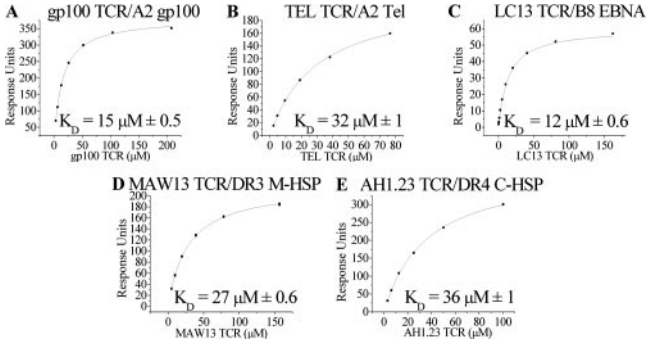

FIGURE 5. Equilibrium-binding analysis at 37°C. *a–c*, TCR-I equilibrium-binding responses to their cognate pMHC-I. *d* and *e*, TCR-II equilibrium-binding responses to their cognate pMHC-II. All TCRs were injected at 37°C and six to eight serial dilutions were conducted in triplicate for each equilibrium experiment. The average response for each concentration is plotted with SD ($n = 3$). The equilibrium-binding constant (K_D) values are plotted using a nonlinear curve fit ($y = (P_1x)/(P_2 + x)$).

Table VI. *Equilibrium analysis data at 37°C*

	K_D μM
TCR-I/pMHC-I	
gp100 TCR/A2 gp100	15 ± 0.5
TEL TCR/A2 Tel	32 ± 1
LC13 TCR/B8 EBNA	12 ± 0.6
TCR-II/pMHC-II	
MAW13 TCR/DR3 M-HSP	27 ± 0.6
AH1.23 TCR/DR4 C-HSP	36 ± 1

K_{off} values fall within a narrow window, which suggests an absolute requirement for a sufficient duration of engagement for TCR-mediated signal transduction (21, 29). Collective knowledge suggests that, on the one hand, TCR binding must be of sufficient duration to allow the molecular events involved in T cell activation to occur. On the other hand, the interactions must be brief enough to allow each Ag complex to be contacted by multiple TCRs (16) and, eventually, enable the T cell to disengage from the target cell. Second, K_{on} values for TCR/pMHC interactions vary widely and account for most of the significantly stronger affinity range observed for TCR-I, compared with TCR-II, interactions. This may reflect that the TCR docking surfaces of most pMHC-II complexes are conformationally more flexible than those of pMHC-I. Thus TCRs, when binding to pMHC-II, may generally incur a higher entropic cost leading to slower on-rates (28, 34, 39, 40). Third, this data indicates that a TCR-affinity hierarchy may exist dependent on Ag origin (pathogenic>tumor/self). This is likely to be the consequence of thymic deletion of higher affinity self-reactive TCRs, leaving the peripheral TCR repertoire with better potential to respond to alien Ags.

Acknowledgments

We thank Scott Burrows, Paul Bowness, Hill Gaston, Marcus Maurer, Brendan Classon, Nikolai Lissin, Ruth Moysey, Nathaniel Liddy, Emma Baston, Brian Cameron, Penio Todorov, and Annelise Vuidepot for making T cell clones, and both TCR and MHC constructs, available for this study.

Disclosures

The authors have no financial conflict of interest.

References

1. Davis, M. M., and P. J. Bjorkman. 1988. T-cell antigen receptor genes and T-cell recognition. *Nature* 334: 395–402.
2. Garcia, K. C., M. Degano, J. A. Speir, and I. A. Wilson. 1999. Emerging principles for T cell receptor recognition of antigen in cellular immunity. *Rev. Immunogenet.* 1: 75–90.
3. Garcia, K. C., M. Degano, R. L. Stanfield, A. Brunmark, M. R. Jackson, P. A. Peterson, L. Teyton, and I. A. Wilson. 1996. An αβ T cell receptor structure at 2.5 A and its orientation in the TCR-MHC complex. *Science* 274: 209–219.
4. Townsend, A., and H. Bodmer. 1989. Antigen recognition by class I-restricted T lymphocytes. *Annu. Rev. Immunol.* 7: 601–624.
5. Reinherz, E. L., K. Tan, L. Tang, P. Kern, J. Liu, Y. Xiong, R. E. Hussey, A. Smolyar, B. Hare, R. Zhang, et al. 1999. The crystal structure of a T cell receptor in complex with peptide and MHC class II. *Science* 286: 1913–1921.
6. Rudolph, M. G., R. L. Stanfield, and I. A. Wilson. 2006. How TCRs bind MHCs, peptides, and coreceptors. *Annu. Rev. Immunol.* 24: 419–466.
7. Saper, M. A., P. J. Bjorkman, and D. C. Wiley. 1991. Refined structure of the human histocompatibility antigen HLA-A2 at 2.6 A resolution. *J. Mol. Biol.* 219: 277–319.
8. Kagi, D., B. Ledermann, K. Burki, R. M. Zinkernagel, and H. Hengartner. 1996. Molecular mechanisms of lymphocyte-mediated cytotoxicity and their role in immunological protection and pathogenesis in vivo. *Annu. Rev. Immunol.* 14: 207–232.
9. Brown, J. H., T. S. Jardetzky, J. C. Gorga, L. J. Stern, R. G. Urban, J. L. Strominger, and D. C. Wiley. 1993. Three-dimensional structure of the human class II histocompatibility antigen HLA-DR1. *Nature* 364: 33–39.
10. Krummel, M. F., M. D. Sjaastad, C. Wulfing, and M. M. Davis. 2000. Differential clustering of CD4 and CD3ζ during T cell recognition. *Science* 289: 1349–1352.
11. Mosmann, T. R., and R. L. Coffman. 1989. TH1 and TH2 cells: different patterns of lymphokine secretion lead to different functional properties. *Annu. Rev. Immunol.* 7: 145–173.
12. Arstila, T. P., A. Casrouge, V. Baron, J. Even, J. Kanellopoulos, and P. Kourilsky. 1999. A direct estimate of the human αβ T cell receptor diversity. *Science* 286: 958–961.
13. Matis, L. A. 1990. The molecular basis of T-cell specificity. *Annu. Rev. Immunol.* 8: 65–82.
14. Rudolph, M. G., J. G. Luz, and I. A. Wilson. 2002. Structural and thermodynamic correlates of T cell signaling. *Annu. Rev. Biophys. Biomol. Struct.* 31: 121–149.
15. Savage, P. A., and M. M. Davis. 2001. A kinetic window constricts the T cell receptor repertoire in the thymus. *Immunity* 14: 243–252.
16. Valitutti, S., S. Muller, M. Cella, E. Padovan, and A. Lanzavecchia. 1995. Serial triggering of many T-cell receptors by a few peptide-MHC complexes. *Nature* 375: 148–151.
17. Viola, A., and A. Lanzavecchia. 1996. T cell activation determined by T cell receptor number and tunable thresholds. *Science* 273: 104–106.
18. van der Merwe, P. A., and S. J. Davis. 2003. Molecular interactions mediating T cell antigen recognition. *Annu. Rev. Immunol.* 21: 659–684.
19. Matsui, K., J. J. Boniface, P. A. Reay, H. Schild, B. Fazekas de St. Groth, and M. M. Davis. 1991. Low affinity interaction of peptide-MHC complexes with T cell receptors. *Science* 254: 1788–1791.
20. Davis, M. M., J. J. Boniface, Z. Reich, D. Lyons, J. Hampl, B. Arden, and Y. Chien. 1998. Ligand recognition by αβ T cell receptors. *Annu. Rev. Immunol.* 16: 523–544.
21. Lyons, D. S., S. A. Lieberman, J. Hampl, J. J. Boniface, Y. Chien, L. J. Berg, and M. M. Davis. 1996. A TCR binds to antagonist ligands with lower affinities and faster dissociation rates than to agonists. *Immunity* 5: 53–61.
22. Garboczi, D. N., P. Ghosh, U. Utz, Q. R. Fan, W. E. Biddison, and D. C. Wiley. 1996. Structure of the complex between human T-cell receptor, viral peptide and HLA-A2. *Nature* 384: 134–141.
23. Boulter, J. M., M. Glick, P. T. Todorov, E. Baston, M. Sami, P. Rizkallah, and B. K. Jakobsen. 2003. Stable, soluble T-cell receptor molecules for crystallization and therapeutics. *Protein Eng.* 16: 707–711.
24. Hennecke, J., A. Carfi, and D. C. Wiley. 2000. Structure of a covalently stabilized complex of a human αβ T-cell receptor, influenza HA peptide and MHC class II molecule, HLA-DR1. *EMBO J.* 19: 5611–5624.
25. Wyer, J. R., B. E. Willcox, G. F. Gao, U. C. Gerth, S. J. Davis, J. I. Bell, P. A. van der Merwe, and B. K. Jakobsen. 1999. T cell receptor and coreceptor CD8 αα bind peptide-MHC independently and with distinct kinetics. *Immunity* 10: 219–225.
26. Borg, N. A., L. K. Ely, T. Beddoe, W. A. Macdonald, H. H. Reid, C. S. Clements, A. W. Purcell, L. Kjer-Nielsen, J. J. Miles, S. R. Burrows, et al. 2005. The CDR3 regions of an immunodominant T cell receptor dictate the "energetic landscape" of peptide-MHC recognition. *Nat. Immunol.* 6: 171–180.
27. Ding, Y. H., B. M. Baker, D. N. Garboczi, W. E. Biddison, and D. C. Wiley. 1999. Four A6-TCR/peptide/HLA-A2 structures that generate very different T cell signals are nearly identical. *Immunity* 11: 45–56.
28. Willcox, B. E., G. F. Gao, J. R. Wyer, J. E. Ladbury, J. I. Bell, B. K. Jakobsen, and P. A. van der Merwe. 1999. TCR binding to peptide-MHC stabilizes a flexible recognition interface. *Immunity* 10: 357–365.
29. McKeithan, T. W. 1995. Kinetic proofreading in T-cell receptor signal transduction. *Proc. Natl. Acad. Sci. USA* 92: 5042–5046.
30. Cole, D. K., and G. F. Gao. 2004. CD8: adhesion molecule, co-receptor and immuno-modulator. *Cell. Mol. Immunol.* 1: 81–88.
31. Kern, P., R. E. Hussey, R. Spoerl, E. L. Reinherz, and H. C. Chang. 1999. Expression, purification, and functional analysis of murine ectodomain fragments of CD8αα and CD8αβ dimers. *J. Biol. Chem.* 274: 27237–27243.
32. Gonzalez, P. A., L. J. Carreno, D. Coombs, J. E. Mora, E. Palmieri, B. Goldstein, S. G. Nathenson, and A. M. Kalergis. 2005. T cell receptor binding kinetics required for T cell activation depend on the density of cognate ligand on the antigen-presenting cell. *Proc. Natl. Acad. Sci. USA* 102: 4824–4829.
33. Purbhoo, M. A., J. M. Boulter, D. A. Price, A. L. Vuidepot, C. S. Hourigan, P. R. Dunbar, K. Olson, S. J. Dawson, R. E. Phillips, B. K. Jakobsen, et al. 2001. The human CD8 coreceptor effects cytotoxic T cell activation and antigen sensitivity primarily by mediating complete phosphorylation of the T cell receptor ζ chain. *J. Biol. Chem.* 276: 32786–32792.
34. Rudolph, M. G., and I. A. Wilson. 2002. The specificity of TCR/pMHC interaction. *Curr. Opin. Immunol.* 14: 52–65.
35. Cole, D. K., P. J. Rizkallah, F. Gao, N. I. Watson, J. M. Boulter, J. I. Bell, M. Sami, G. F. Gao, and B. K. Jakobsen. 2006. Crystal structure of HLA-A*2402 complexed with a telomerase peptide. *Eur. J. Immunol.* 36: 170–179.
36. Hemmer, B., B. T. Fleckenstein, M. Vergelli, G. Jung, H. McFarland, R. Martin, and K. H. Wiesmuller. 1997. Identification of high potency microbial and self ligands for a human autoreactive class II-restricted T cell clone. *J. Exp. Med.* 185: 1651–1659.
37. Wilson, D. B., D. H. Wilson, K. Schroder, C. Pinilla, S. Blondelle, R. A. Houghten, and K. C. Garcia. 2004. Specificity and degeneracy of T cells. *Mol. Immunol.* 40: 1047–1055.
38. Davis, M. M., D. S. Lyons, J. D. Altman, M. McHeyzer-Williams, J. Hampl, J. J. Boniface, and Y. Chien. 1997. T cell receptor biochemistry, repertoire selection and general features of TCR and Ig structure. *Ciba Found. Symp.* 204: 94–100; discussion 100–104.
39. Garcia, K. C., M. Degano, L. R. Pease, M. Huang, P. A. Peterson, L. Teyton, and I. A. Wilson. 1998. Structural basis of plasticity in T cell receptor recognition of a self peptide-MHC antigen. *Science* 279: 1166–1172.
40. Boniface, J. J., Z. Reich, D. S. Lyons, and M. M. Davis. 1999. Thermodynamics of T cell receptor binding to peptide-MHC: evidence for a general mechanism of molecular scanning. *Proc. Natl. Acad. Sci. USA* 96: 11446–11451.

41. Sykulev, Y., A. Brunmark, M. Jackson, R. J. Cohen, P. A. Peterson, and H. N. Eisen. 1994. Kinetics and affinity of reactions between an antigen-specific T cell receptor and peptide-MHC complexes. *Immunity* 1: 15–22.
42. Alam, S. M., P. J. Travers, J. L. Wung, W. Nasholds, S. Redpath, S. C. Jameson, and N. R. Gascoigne. 1996. T-cell-receptor affinity and thymocyte positive selection. *Nature* 381: 616–620.
43. Arcaro, A., C. Gregoire, T. R. Bakker, L. Baldi, M. Jordan, L. Goffin, N. Boucheron, F. Wurm, P. A. van der Merwe, B. Malissen, and I. F. Luescher. 2001. CD8β endows CD8 with efficient coreceptor function by coupling T cell receptor/CD3 to raft-associated CD8/p56^{lck} complexes. *J. Exp. Med.* 194: 1485–1495.
44. Reiser, J. B., C. Darnault, A. Guimezanes, C. Gregoire, T. Mosser, A. M. Schmitt-Verhulst, J. C. Fontecilla-Camps, B. Malissen, D. Housset, and G. Mazza. 2000. Crystal structure of a T cell receptor bound to an allogeneic MHC molecule. *Nat. Immunol.* 1: 291–297.
45. Kersh, G. J., E. N. Kersh, D. H. Fremont, and P. M. Allen. 1998. High- and low-potency ligands with similar affinities for the TCR: the importance of kinetics in TCR signaling. *Immunity* 9: 817–826.
46. Garcia, K. C., C. G. Radu, J. Ho, R. J. Ober, and E. S. Ward. 2001. Kinetics and thermodynamics of T cell receptor-autoantigen interactions in murine experimental autoimmune encephalomyelitis. *Proc. Natl. Acad. Sci. USA* 98: 6818–6823.
47. Chen, J. L., G. Stewart-Jones, G. Bossi, N. M. Lissin, L. Wooldridge, E. M. Choi, G. Held, P. R. Dunbar, R. M. Esnouf, M. Sami, et al. 2005. Structural and kinetic basis for heightened immunogenicity of T cell vaccines. *J. Exp. Med.* 201: 1243–1255.
48. Tynan, F. E., N. A. Borg, J. J. Miles, T. Beddoe, D. El-Hassen, S. L. Silins, W. J. van Zuylen, A. W. Purcell, L. Kjer-Nielsen, J. McCluskey, et al. 2005. High resolution structures of highly bulged viral epitopes bound to major histocompatibility complex class I. Implications for T-cell receptor engagement and T-cell immunodominance. *J. Biol. Chem.* 280: 23900–23909.
49. Lee, J. K., G. Stewart-Jones, T. Dong, K. Harlos, K. Di Gleria, L. Dorrell, D. C. Douek, P. A. van der Merwe, E. Y. Jones, and A. J. McMichael. 2004. T cell cross-reactivity and conformational changes during TCR engagement. *J. Exp. Med.* 200: 1455–1466.
50. Burrows, S. R., R. A. Elkington, J. J. Miles, K. J. Green, S. Walker, S. M. Haryana, D. J. Moss, H. Dunckley, J. M. Burrows, and R. Khanna. 2003. Promiscuous CTL recognition of viral epitopes on multiple human leukocyte antigens: biological validation of the proposed HLA A24 supertype. *J. Immunol.* 171: 1407–1412.
51. Burrows, S. R., S. J. Rodda, A. Suhrbier, H. M. Geysen, and D. J. Moss. 1992. The specificity of recognition of a cytotoxic T lymphocyte epitope. *Eur. J. Immunol.* 22: 191–195.
52. Cox, A. L., J. Skipper, Y. Chen, R. A. Henderson, T. L. Darrow, J. Shabanowitz, V. H. Engelhard, D. F. Hunt, and C. L. Slingluff, Jr. 1994. Identification of a peptide recognized by five melanoma-specific human cytotoxic T cell lines. *Science* 264: 716–719.
53. Moss, P. A., R. J. Moots, W. M. Rosenberg, S. J. Rowland-Jones, H. C. Bodmer, A. J. McMichael, and J. I. Bell. 1991. Extensive conservation of α and β chains of the human T-cell antigen receptor recognizing HLA-A2 and influenza A matrix peptide. *Proc. Natl. Acad. Sci. USA* 88: 8987–8990.
54. Roman, G. C., and M. Osame. 1988. Identity of HTLV-I-associated tropical spastic paraparesis and HTLV-I-associated myelopathy. *Lancet* 1: 651.
55. Bowness, P., R. L. Allen, and A. J. McMichael. 1994. Identification of T cell receptor recognition residues for a viral peptide presented by HLA B27. *Eur. J. Immunol.* 24: 2357–2363.
56. Bowness, P., R. L. Allen, D. N. Barclay, E. Y. Jones, and A. J. McMichael. 1998. Importance of a conserved TCR J α-encoded tyrosine for T cell recognition of an HLA B27/peptide complex. *Eur. J. Immunol.* 28: 2704–2713.
57. Deane, K. H., R. M. Jecock, J. H. Pearce, and J. S. Gaston. 1997. Identification and characterization of a DR4-restricted T cell epitope within chlamydia heat shock protein 60. *Clin. Exp. Immunol.* 109: 439–445.
58. Lamb, J. R., D. D. Eckels, M. Phelan, P. Lake, and J. N. Woody. 1982. Antigen-specific human T lymphocyte clones: viral antigen specificity of influenza virus-immune clones. *J. Immunol.* 128: 1428–1432.
59. Mertz, A. K., P. Wu, T. Sturniolo, D. Stoll, M. Rudwaleit, R. Lauster, J. Braun, and J. Sieper. 2000. Multispecific CD4$^+$ T cell response to a single 12-mer epitope of the immunodominant heat-shock protein 60 of *Yersinia enterocolitica* in *Yersinia*-triggered reactive arthritis: overlap with the B27-restricted CD8 epitope, functional properties, and epitope presentation by multiple DR alleles. *J. Immunol.* 164: 1529–1537.
60. Wucherpfennig, K. W., K. Ota, N. Endo, J. G. Seidman, A. Rosenzweig, H. L. Weiner, and D. A. Hafler. 1990. Shared human T cell receptor Vβ usage to immunodominant regions of myelin basic protein. *Science* 248: 1016–1019.